



Automated fitting of thermogravimetric analysis data

Morgan C. Bruns¹ | Isaac T. Leventon²

¹Department of Mechanical Engineering,
Virginia Military Institute, Lexington, Virginia

²Fire Research Division, National Institute of
Standards and Technology, Gaithersburg,
Maryland

Correspondence

Morgan C. Bruns, Department of Mechanical
Engineering, Virginia Military Institute,
710 Nichols Hall, Lexington, VA 24450.
Email: morgan.chase.bruns@gmail.com

Summary

A novel methodology has been developed for extracting pyrolysis kinetic parameters from thermogravimetric analysis (TGA) data. The development of this methodology is motivated by a need to automate the determination of material properties for use in fire models. The algorithm with which the methodology is implemented is described. Aside from being fully automated, the resultant script has the advantage of being efficient—a full set of kinetic parameters is provided in less than 1 second. The script is verified against manufactured TGA data for one and two reaction mechanisms and the effects of reaction peak width and the distance between reaction peaks is examined. Validation is accomplished by applying the script to TGA data for Nylon 6,6, a flexible polyurethane foam, and polyvinyl chloride. The resultant kinetic parameters are tabulated, and plots of the actual and predicted TGA data show that the algorithm is quite effective for one, two, and three reaction mechanisms.

KEYWORDS

fire modeling, kinetics, nylon 6,6, polyurethane foam, polyvinyl chloride, pyrolysis, TGA

1 | INTRODUCTION

Computational fire models have proven to be effective at predicting the spread of heat and smoke in a wide range of building fire scenarios. However, such models still generally require user input describing the actual fire that is generating the heat and smoke. Computational predictions of flame spread and fire growth require somewhat detailed models of condensed phase physics, and a number of condensed phase pyrolysis models have been developed.^{1–3} Such models have proven effective at modeling the burning rate of small slabs, but their application to flame spread calculations is more limited. Part of the problem is that these pyrolysis models require the specification of a large number of material properties. Furthermore, there are many different flammable materials that need to be considered in fire scenarios. Substantial progress in applying computational fire models to predict flame spread could be achieved by the development of both a streamlined methodology for characterizing the thermophysical properties of flammable materials as well as the creation of a publicly available database of such material properties.

One successful approach for characterizing materials is based on performing a number of milligram-scale and bench scale tests such as thermogravimetric analysis (TGA), differential scanning calorimetry (DSC), and the controlled atmosphere pyrolysis apparatus.⁴ An example of a public database of material properties is found in the Validation Guide of the Fire Dynamics Simulator (FDS).⁵ Currently, an international effort is underway to further develop experimental and modeling tools such as these in order to “advance predictive fire modelling”.⁶ The present manuscript presents work based on a coordinated effort to develop a comprehensive database of material properties for use in fire models. This database will include both raw data from a suite of milligram-scale tests and a list of properties for each material that could be directly used as inputs for a fire model such as FDS. In order to generate these tables of material properties, automated computational scripts are required to robustly analyze raw data from small-scale tests. In this paper, we present such a script for calibrating a generalized pyrolysis kinetic model to TGA data. Previous work has looked at optimization algorithms⁷ and Markov Chain Monte Carlo methods⁸ for fitting TGA data, but these approaches are not fully automated for general multistep reaction schemes and can be relatively computationally expensive.

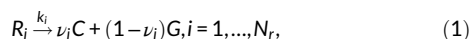
This article has been contributed to by US Government employees and their work is in the public domain in the USA.

2 | THEORY

In TGA, the mass of a small sample of material is measured while heated according to a prescribed temperature program. Typically, the sample will be heated at a constant temperature ramp rate. If the sample mass and heating rate are sufficiently small, then the temperature and composition throughout the sample are approximately uniform. As the material is heated, chemical bonds are broken producing smaller molecules. Eventually, the products of pyrolysis become small enough to vaporize, and mass is lost from the system. Models of this process typically take the form of a system of reactions with unimolecular Arrhenius kinetics.

2.1 | Independent Unimolecular Reactions

In the following, focus is limited to systems of independent reactions. This generalized model could account for (a) a system of parallel reactions or (b) a system of series reactions in which the subsequent reactions occur at different temperatures. To begin, consider a system of N_r unimolecular reactions of the form



where R_i is the label for the reactant material, C is the label for the condensed phase products of the reaction, k_i is the reaction rate constant, ν_i is the residual mass fraction of the reaction, and G is the label for the gas species which escapes the sample. For the purposes of the following analysis, it is not necessary to distinguish between the condensed phase and gas phase products of the reactions. Additionally, consideration will be limited to constant heating rate TGA experiments in which the sample temperature increases at a constant rate, β . An Arrhenius model is assumed for the temperature dependence of the rate constant such that, for each reaction

$$k_i = \left(\frac{A_i}{\beta}\right) \exp\left(-\frac{E_i}{RT}\right), \quad (2)$$

where A_i is the pre-exponential, E_i is the activation energy, and R is the gas constant. Note that the heating rate has been directly absorbed into the rate constant in order to simplify the notation in the following analysis. Consequently, k_i is not strictly speaking the Arrhenius rate constant, but the kinetic pair (A_i, E_i) are the true Arrhenius pre-exponential and activation energy, respectively.

For the kinetic model described by Equations (1), the temperature rate of change of the mass of component i , m_i , is governed by

$$m'_i \equiv \frac{dm_i}{dT} = -m_i k_i, \quad (3)$$

along with the initial condition $m_i(T_0) = m_{0,i}$ where T_0 is the initial temperature of the TGA experiment (or any temperature prior to the

onset of the reaction). The total sample mass of the sample is simply the sum of the individual component masses. The total mass loss rate must account for the generation of residual solid products of the reactions so that

$$m' \equiv \frac{dm}{dT} = \sum_i (1 - \nu_i) m'_i. \quad (4)$$

2.2 | Nondimensional form and approximate solution

It is convenient to nondimensionalize Equation (3), and the resultant nondimensionalization leads to an approximate solution which is valid for most materials. The peak mass loss rate may be found by differentiating Equation (3) with respect to temperature and setting the result equal to zero. Analysis of this peak condition yields the following results. Using $T_{p,i}$, $m_{p,i}$, and $m'_{p,i}$ to denote the temperature, mass, and temperature derivative of the mass corresponding to that peak, a characteristic width of the peak may be defined as

$$\Delta T_i \equiv \frac{-m_{p,i}}{m'_{p,i}} = \frac{RT_{p,i}^2}{E_i}, \quad (5)$$

where the second equality in Equation (5) is determined from analysis of the peak equation. The kinetic equations can be recast in terms of the peak temperature and the peak width parameters which are related to the Arrhenius parameters through

$$E_i = \frac{RT_{p,i}^2}{\Delta T_i}. \quad (6)$$

$$A_i = \frac{\beta}{\Delta T_i} \exp\left(\frac{T_{p,i}}{\Delta T_i}\right). \quad (7)$$

A simplified form of the kinetic equations may be obtained using the following nondimensionalization

$$\mu_i \equiv \frac{m_i}{m_{0,i}}. \quad (8)$$

$$\theta_i \equiv \frac{T - T_{p,i}}{\Delta T_i}. \quad (9)$$

The nondimensional kinetic equation for component i becomes

$$\mu'_i \equiv \frac{d\mu_i}{d\theta_i} = -\mu_i \exp\left(\frac{\theta_i}{\xi_i \theta_i + 1}\right), \quad (10)$$

with the boundary condition $\mu_i(\theta_i \rightarrow -\infty) = 1$ where $\xi_i \equiv \Delta T_i / T_{p,i}$, i may be thought of as a shape parameter for the mass loss peak.

For the limiting case in which $\xi_i \rightarrow 0$, Equation (10) has the exact solution:

$$\mu_i = \exp[-\exp(\theta_i)], \quad (11)$$

or, in dimensional form,

$$m_i = m_{0,i} \exp \left[-\exp \left(\frac{T - T_{p,i}}{\Delta T_i} \right) \right]. \quad (12)$$

Note that Equation (12) predicts that that mass at the peak rate of temperature change is $m_{0,i} e^{-1}$ which is the same approximation derived by other authors.⁹ Furthermore, the assumption of letting $\xi_i \rightarrow 0$ is equivalent to $RT_{p,i} \ll E_i$ which is the same assumption used to arrive at this approximation.

2.3 | Reaction Peak Analysis

Equation (12) may be used in conjunction with TGA data to get estimates of the kinetic parameters. The approach developed in the following makes use of the fact that if the peak temperatures, $T_{p,i}$, are known from the data, it is possible to use derivatives of Equation (12) to obtain estimates of ΔT_i and the total mass lost from the sample due to the reaction, Δm_i , from the data. Note that the total mass change associated with a reaction is

$$\Delta m_i \equiv m_{0,i}(1 - \nu_i). \quad (13)$$

Taking the first three derivatives with respect to temperature of Equation (12) results in:

$$d_{1,i} \equiv (1 - \nu_i) m_i' = \frac{\Delta m_i}{\Delta T_i} g_i \exp(g_i), \quad (14)$$

$$d_{2,i} \equiv (1 - \nu_i) m_i'' = \frac{\Delta m_i}{\Delta T_i^2} g_i \exp(g_i) (g_i + 1), \quad (15)$$

$$d_{3,i} \equiv (1 - \nu_i) m_i''' = \frac{\Delta m_i}{\Delta T_i^3} g_i \exp(g_i) (g_i^2 + 3g_i + 1), \quad (16)$$

where

$$g_i \equiv -\exp \left(\frac{T - T_{p,i}}{\Delta T_i} \right). \quad (17)$$

Note that the newly defined d -variables in Equations (14) to (16) represent the contribution of each component to the first three temperature derivatives of the total mass. Thus,

$$m' = \sum_i d_{1,i}. \quad (18)$$

$$m'' = \sum_i d_{2,i}. \quad (19)$$

$$m''' = \sum_i d_{3,i}. \quad (20)$$

At the peak temperature, $g_i = -1$, and so Equations (14) to (16) yield

$$d_{1,i}(T_{p,i}) = -\frac{\Delta m_i}{e \Delta T_i}. \quad (21)$$

$$d_{2,i}(T_{p,i}) = 0. \quad (22)$$

$$d_{3,i}(T_{p,i}) = \frac{\Delta m_i}{e \Delta T_i^3}. \quad (23)$$

Equation (22) shows that the peak condition is in fact being satisfied. The solution of Equations (21) and (23) in gives

$$\Delta T_i = \sqrt{-\frac{d_{1,i}(T_{p,i})}{d_{3,i}(T_{p,i})}}, \quad (24)$$

$$\Delta m_i = -e d_{1,i}(T_{p,i}) \Delta T_i, \quad (25)$$

where using Equations (18) and (20),

$$d_{1,i}(T_{p,i}) = m'(T_{p,i}) - \sum_{j \neq i} d_{1,j}(T_{p,i}). \quad (26)$$

$$d_{3,i}(T_{p,i}) = m'''(T_{p,i}) - \sum_{j \neq i} d_{3,j}(T_{p,i}). \quad (27)$$

In the following section, an algorithm is presented for using Equations (24) to (27) in conjunction with TGA data to obtain a set of kinetic parameters.

2.4 | Description of algorithm

In order to use Equations (24) to (27), it is necessary to have the temperature derivatives of the TGA data. That is, given the set of TGA data points for (T, m) , what are the corresponding values of m' , m'' , and m''' at each temperature? It was found that the Savitzky-Golay filter¹⁰ proved to be effective in estimating the derivatives of noisy TGA data. Application of the Savitzky-Golay filter requires two parameters: (a) the order of the polynomial fit and (b) the number of data points used in the fit. A quadratic fit was used for the first temperature derivative, a cubic fit for the second derivative, and a quartic fit was used for the third derivative data. The number of data points used in the fit was chosen to be enough to cover a temperature window of 10 K for the first temperature derivative, 20 K for the second derivative, and 40 K for the third derivative. These parameters were determined by trial and error, and future work will examine optimizing the choice of these parameters.

Once the first 3 derivatives of the TGA mass data were determined, it is necessary to determine the number of reactions. Clear reaction peaks correspond to points at which $m'' = 0$ and $m''' > 0$. All

such peaks are easily obtained from the filtered temperature derivatives. Only peaks in which the mass loss rate was greater than 15% of the maximum peak mass loss rate were identified as distinct reactions. If two reactions occur over similar temperature ranges, it is often difficult to observe a distinct peak in the mass loss rate. However, in some cases the presence of a shoulder in the peak is evidence of a partially obscured reaction. Partially obscured reactions were found by locating points where m'' is small and $m''' = 0$.

The preceding paragraph presents two criteria for identifying reaction peaks. Each of these points corresponds to a temperature at which the peak occurs. So at this point in the algorithm, all that is stored is a set of N_r temperatures, $T_{p,i}$ for $i = 1, \dots, N_r$. The next step is to determine the kinetic parameters for each of these reactions.

For the single reaction case, the total volatile mass lost from the reaction is equal to the total mass lost by the TGA sample, or

$$\Delta m_1 = \Delta m_{\text{tot}} \equiv m_0 - m_f, \quad (28)$$

where m_0 and m_f are the initial and final masses of the sample. With only one reaction, Equation (26) gives

$$d_{1,1}(T_{p,1}) = m'(T_{p,1}), \quad (29)$$

and so, upon substitution into and rearrangement of Equation (25),

$$\Delta T_1 = -\frac{\Delta m_{\text{tot}}}{em'(T_{p,1})}. \quad (30)$$

If more than one peak is found, the process is complicated since the mass loss rate signals can overlap. An iterative approach has been developed in which an initial guess of all Δm_i and ΔT_i are used to compute Equations (26) and (27), and then the resultant values are used in Equations (24) and (25) to find updated values for these kinetic parameters. The process is repeated until convergence is achieved.

An important correction must be employed to insure that $\sum_i \Delta m_i = \Delta m_{\text{tot}}$. Using Equations (24) and (25) for each reaction separately does not guaranty that this condition will be satisfied. In order, to identify a mass conserving mechanism an intermediate solution ΔT_i^* is found from Equation (24). The mass conserving peak widths would be those which satisfy:

$$\Delta m_{\text{tot}} = \sum_i -ed_{1,i}(T_{p,i})\Delta T_i. \quad (31)$$

The projection of the intermediate solution onto the space of solutions satisfying Equation (31) is found by:

$$\Delta \mathbf{T} = \Delta \mathbf{T}^* - \left(\frac{\Delta \mathbf{T}^* \cdot \mathbf{a} - \Delta m_{\text{tot}}}{\mathbf{a} \cdot \mathbf{a}} \right) \mathbf{a}, \quad (32)$$

where $\Delta \mathbf{T}^*$ and $\Delta \mathbf{T}$ are simply the vectors formed from the temperature widths for the intermediate and mass conserving cases, and \mathbf{a} is the vector whose elements are $a_i \equiv -ed_{1,i}(T_{p,i})$. The mass widths for

an iteration are then found from the mass conserving temperature widths used in Equation (25).

The entire algorithm for finding the kinetic parameters of TGA data indicating several reactions is summarized as follows:

- 1 Estimate reaction mass changes using $\Delta m_i = \Delta m_{\text{tot}}/N_r$ for each i .
- 2 Compute corresponding estimates of peak widths using $\Delta T_i = -\Delta m_i/em(T_{p,i})$ for each i .
- 3 Compute $d_{1,i}$ and $d_{3,i}$ for each i using the previously determined values for Δm_i and ΔT_i .
- 4 Find initial estimates ΔT_i^* for each i using Equation (24).
- 5 Calculate mass conserving temperature widths using Equation (32).
- 6 Calculate mass conserving reaction mass changes using Equation (25).
- 7 Repeat steps 3 through 6 until Δm_i and ΔT_i converge.

It was found that even for the most complex scenarios considered that convergence was achieved after approximately 10 to 20 iterations making the algorithm extremely efficient. In the next two sections, the algorithm described in this section will be verified against manufactured data and validated against TGA data for several materials. In all cases, the algorithm requires less than 1 second of CPU time on a typical laptop computer to provide the complete set of kinetic parameters.

3 | VERIFICATION

It is possible to verify the algorithm described in the preceding section by testing it against numerically generated TGA data based on an assumed kinetic model. In this process, TGA data is manufactured by simulating a solution of Equation (4) using assumed parameter values. The algorithm was then applied to this manufactured data. The resultant calibrated kinetic parameters can be compared to the specified value, and predictions using the calibrated kinetic parameters can be compared to the manufactured data. In all cases, a heating rate of 10 K/minute was used along with an initial sample mass of $m_0 = 1$.

3.1 | One reaction

Three single-reaction cases have been considered. Each of these three cases specify a peak reaction rate temperature at 650 K, and the sample was assumed to fully volatilize so that $m_f = 0$ and $\Delta m = 1$. In order to examine the effectiveness of the algorithm to handle a variety of data, three different characteristic peak widths were considered: $\Delta T = 10$ K, $\Delta T = 20$ K, and $\Delta T = 40$ K. The specified and calibrated parameters for these three cases are shown in Tables 1 to 3. Plots of the TGA mass and mass loss rate for the three cases are shown in Figure 1. It is clear that the quality of the calibrated reaction decreases with increasing reaction width. This observation is likely a consequence of the fact that the fitting algorithm is based upon an approximate solution of the kinetic equations that assumes a small value of $\xi \equiv \Delta T/T_p$. As the value of ΔT increases, so does the value of ξ , and thus the validity of the approximation decreases.

TABLE 1 Kinetic parameters for the single-reaction verification case with $\Delta T = 10$ K

Kinetic parameter	Specified value	Calibrated value
T_p (K)	650	649.4
ΔT (K)	10	9.99
ξ	0.01538	0.01539
$\ln[A$ (s^{-1})]	60.91	60.90
E (kJ/kmol)	351.3×10^3	350×10^3

TABLE 2 Kinetic parameters for single-reaction verification case with $\Delta T = 20$ K

Kinetic parameter	Specified value	Calibrated value
T_p (K)	650	649.4
ΔT (K)	20	19.07
ξ	0.03077	0.02935
$\ln[A$ (s^{-1})]	27.71	29.34
E (kJ/kmol)	175.6×10^3	184.1×10^3

TABLE 3 Kinetic parameters for single-reaction verification case with $\Delta T = 40$ K

Kinetic parameter	Specified value	Calibrated value
T_p (K)	650	649.4
ΔT (K)	40	36.
ξ	0.06154	0.05563
$\ln[A$ (s^{-1})]	10.77	12.59
E (kJ/kmol)	87.8×10^3	97.1×10^3

3.2 | Two reactions

Three 2-reaction cases were also considered. For these cases, the effect of overlapping peaks was studied. For these scenarios, both reactions are assigned a characteristic peak width of 15 K. The

TABLE 4 Kinetic parameters for two-reaction verification case with $T_{p,2} - T_{p,1} = 160$ K

Kinetic parameter	Specified value	Calibrated value
$T_{p,1}$ (K)	570	569.7
$T_{p,2}$ (K)	730	729.6
ΔT_1 (K)	15	14.12
ΔT_2 (K)	15	15.25
ξ_1	0.02632	0.02478
ξ_2	0.02055	0.02090
Δm_1	0.5	0.4874
Δm_2	0.3	0.3126
$\ln[A_1$ (s^{-1})]	33.50	35.91
$\ln[A_2$ (s^{-1})]	44.17	43.34
E_1 (kJ/kmol)	180.1×10^3	191.1×10^3
E_2 (kJ/kmol)	295.4×10^3	290.2×10^3

normalized mass change associated with the first reaction is $\Delta m_1 = 0.5$, and that of the second reaction is $\Delta m_2 = 0.3$. In all cases, the midpoint between the two reaction peaks is 650 K. The difference between the cases is the distance between the peak temperatures. Three peak temperature differences were considered: 160, 80, and 40 K. The specified and calibrated parameters for these three cases are shown in Tables 4 to 6. Plots of the results of these three verification cases are shown in Figure 2. It is apparent that the algorithm captures the TGA signal well even as the peaks move close together. Although the plateau in the mass signal is overestimated, the mass loss rates are well captured—this is a consequence of the algorithm favoring mass loss rate matching over mass matching.

4 | VALIDATION

The manufactured TGA data considered above represent an idealization of the complex processes actually occurring during the pyrolysis

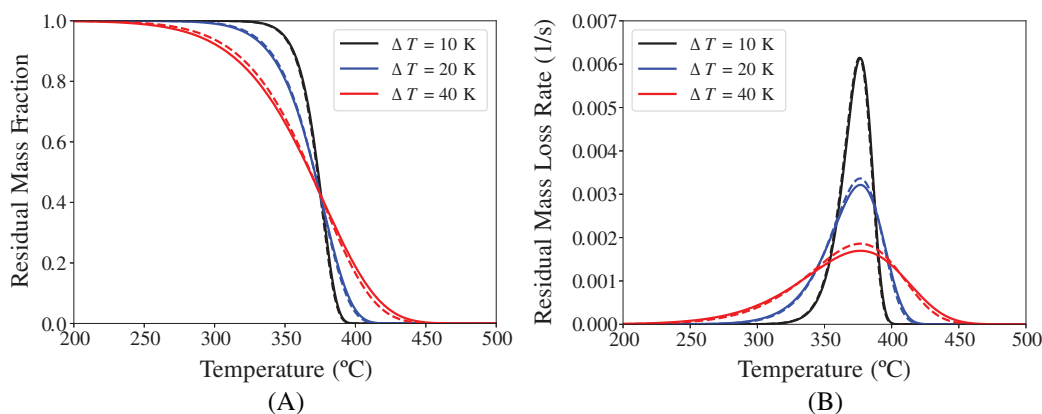
**FIGURE 1** Specified and calibrated TGA (A) normalized mass and (B) normalized mass loss rates for single-reaction verification cases. The solid lines represent the manufactured data and the dashed lines represent model predictions

TABLE 5 Kinetic parameters for two-reaction verification case with $T_{p,2} - T_{p,1} = 80$ K

Kinetic parameter	Specified value	Calibrated value
$T_{p,1}$ (K)	610	609.7
$T_{p,2}$ (K)	690	689.7
ΔT_1 (K)	15	14.20
ΔT_2 (K)	15	15.26
ξ_1	0.02459	0.02329
ξ_2	0.02174	0.02212
Δm_1	0.5	0.4865
Δm_2	0.3	0.3135
$\ln[A_1 (s^{-1})]$	36.17	38.49
$\ln[A_2 (s^{-1})]$	41.50	40.69
E_1 (kJ/kmol)	206.2×10^3	217.6×10^3
E_2 (kJ/kmol)	263.9×10^3	259.3×10^3

TABLE 6 Kinetic parameters for two-reaction verification case with $T_{p,2} - T_{p,1} = 40$ K

Kinetic parameter	Specified value	Calibrated value
$T_{p,1}$ (K)	630	631.2
$T_{p,2}$ (K)	670	669.6
ΔT_1 (K)	15	14.10
ΔT_2 (K)	15	16.59
ξ_1	0.02381	0.02234
ξ_2	0.02239	0.02477
Δm_1	0.5	0.4590
Δm_2	0.3	0.3410
$\ln[A_1 (s^{-1})]$	37.50	40.32
$\ln[A_2 (s^{-1})]$	40.17	35.77
E_1 (kJ/kmol)	220.0×10^3	234.9×10^3
E_2 (kJ/kmol)	248.8×10^3	224.7×10^3

TABLE 7 Calibrated kinetic parameters for Nylon 6,6

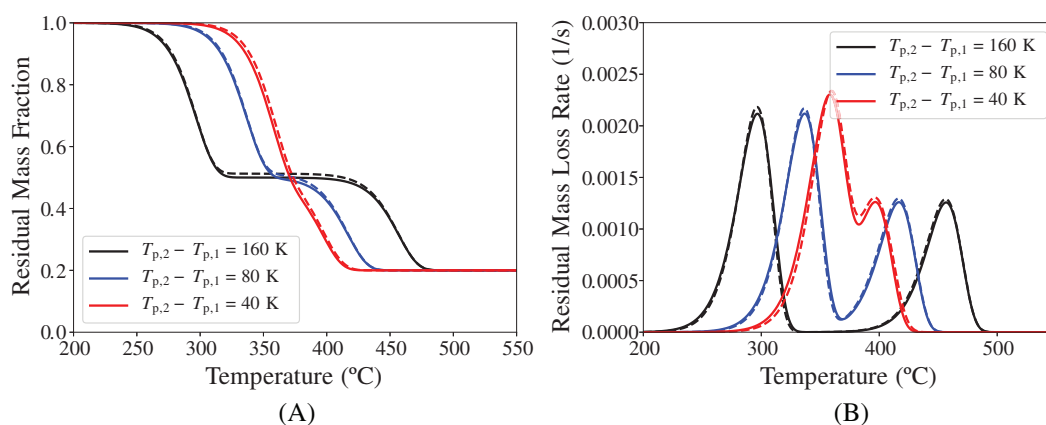
Kinetic parameter	Reaction 1
T_p (K)	716.3
ΔT (K)	22.11
Δm	0.9754
ξ	0.03087
$\ln[A (s^{-1})]$	27.50
E (kJ/kmol)	192.9×10^3

of real materials. It is therefore important to assess the validity of the fitting algorithm against real TGA data.

In this work, TGA experiments were conducted on three polymers: Polyamide 6,6 (Nylon 6,6), a flexible polyurethane (PU) foam, and polyvinyl chloride (PVC). These materials are widely used in construction, residential, and transportation applications, and, collectively, they present a diverse range of decomposition behaviors (eg. single or multiple reaction peaks, discrete or overlapping reactions, and decomposition across a wide temperature range).

TGA experiments were conducted on these three materials in a Netzsch STA 449 F1 Jupiter. This apparatus continuously measures mass (using a microbalance with a 0.025 μ g precision) and temperature (using an S-type thermocouple positioned directly beneath the sample crucible) of samples as they are heated through a well-defined temperature program in an anaerobic environment. A temperature calibration was conducted as per the manufacturer's recommendations¹¹ (using a set of 6 pure metals, with melting points between 156.6 and 961.8°C) to provide a relation between measured and actual sample temperature. The calibration was performed using the same crucible type, heating rate, and gaseous environment as was used during thermal analysis experiments on the polymeric samples. All TGA experiments were conducted within 3 months of this calibration.

The temperature program used for TGA experiments included an initial isotherm at an elevated temperature (below 100°C), during

**FIGURE 2** Specified and calibrated TGA (A) normalized mass and (B) normalized mass loss rate for two-reaction verification cases. The solid lines represent the manufactured data and the dashed lines represent model predictions

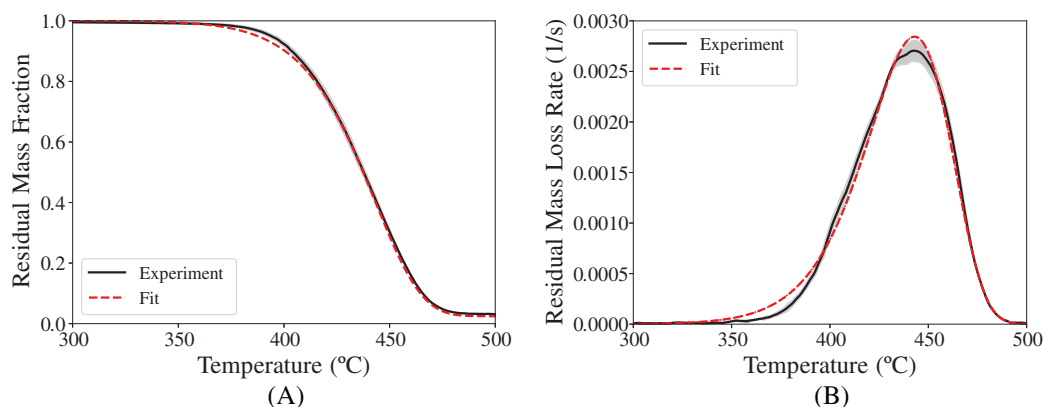


FIGURE 3 Experimental and calibrated TGA (A) normalized mass and (B) normalized mass loss rate for Nylon 6,6. The gray area represents \pm two SDs about the average mass

TABLE 8 Calibrated kinetic parameters for polyurethane foam

Kinetic parameter	Reaction 1	Reaction 2
T_p (K)	562.7	648.5
ΔT (K)	14.50	13.69
Δm	0.2511	0.7280
ξ	0.02577	0.02112
$\ln[A \text{ (s}^{-1}\text{)}]$	34.34	42.95
E (kJ/kmol)	181.5×10^3	255.3×10^3

TABLE 9 Calibrated kinetic parameters for polyvinyl chloride

Kinetic parameter	Reaction 1	Reaction 2	Reaction 3
T_p (K)	568.5	731.7	588.1
ΔT (K)	12.15	22.39	9.62
Δm	0.4200	0.2238	0.1999
ξ	0.02138	0.03060	0.01636
$\ln[A \text{ (s}^{-1}\text{)}]$	42.49	27.78	57.06
E (kJ/kmol)	221.1×10^3	198.8×10^3	298.8×10^3

which time the chamber was continuously purged with nitrogen. This ensured that the system was completely free of oxygen and that any residual moisture in samples was removed prior to dynamic heating and thermal decomposition. Following this conditioning period, samples were heated at a constant rate of 10 K/min up to 700 or 900°C. Throughout this program, the test chamber was continuously purged with ultra-high purity (UHP) nitrogen at 50 mL/min. All tests were conducted in open alumina crucibles.

At the start of each day of testing, a baseline test was performed in which an empty alumina crucible was subjected to the

same heating program as was used during the thermal analysis experiments. This baseline history (mass vs temperature) was subtracted from the corresponding data obtained during experiments on the polymeric samples. All TGA measurement data presented in this work has been baseline-corrected in this manner. All samples were stored in a desiccator (in the presence of Drierite) for a minimum of 48 hours prior to testing. Immediately before testing, samples were removed from the desiccator, placed into alumina test crucibles, and weighed using a Mettler M3 analytical balance.

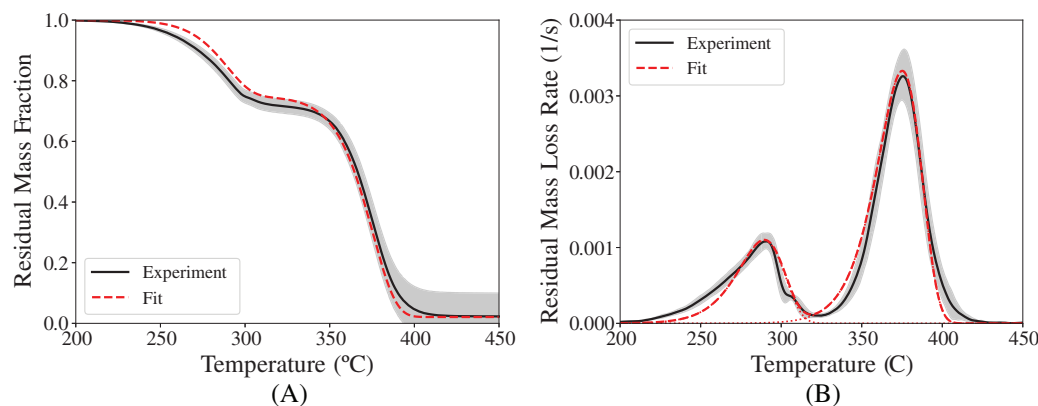


FIGURE 4 Experimental and calibrated TGA (A) normalized mass and (B) normalized mass loss rate for polyurethane foam. The gray area represents \pm two SDs about the average mass

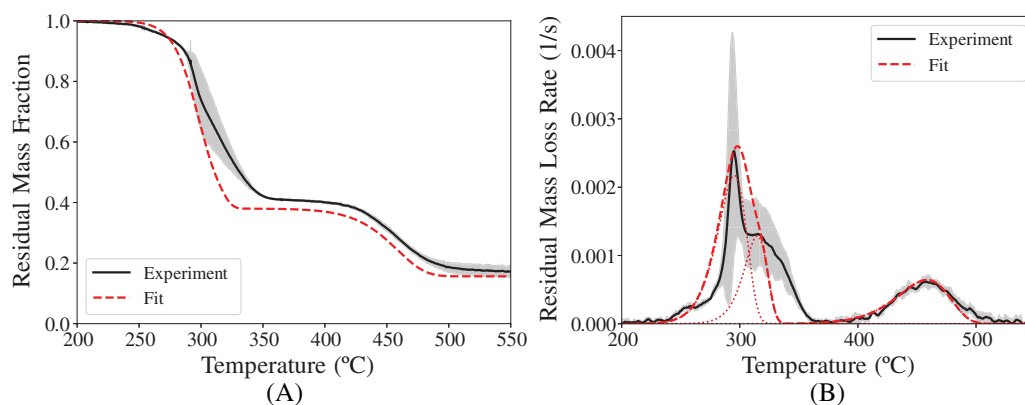


FIGURE 5 Experimental and calibrated TGA (A) normalized mass and (B) normalized mass loss rate for polyvinyl chloride. The gray area represents \pm two SDs about the average mass

4.1 | Polyamide 6,6 (Nylon 6,6)

Polyamide 6,6 (Nylon 6,6) samples were obtained from Goodfellow (Reference number AM323100) in the form of injection molded slabs, which were then cryogenically ground to obtain a powder for testing. For each test, between 4.5 and 5.5 mg of this powder was weighed and then pressed flat into the base of an alumina test crucible. The temperature program included a 20-minute-long isotherm at 27°C followed by heating at a constant rate of 10 K/min to 900°C. Three replicate tests were performed, and the average mass data was used by the algorithm to determine pyrolysis kinetics.

The calibrated kinetic parameters are listed in Table 7. Plots of the TGA data and the fit resulting from the calibrated parameters are provided in Figure 3 along with a gray area representing \pm two standard deviations of the mass data about the average mass. Although the initial onset temperature and the peak mass loss rate are slightly overpredicted, the predicted TGA agrees quite well with the experimental data.

4.2 | Flexible PU Foam

PU foam samples were produced by Innocor Foam Technologies to meet the specifications of a “Standard Polyurethane Foam Substrate” described in ASTM-D3574-08.¹² This foam was purchased in the form of 8 cm thick slabs. Samples used for testing were cut from the center of these slabs into small, cylindrical pieces, between 3.0 and 5.0 mg in mass. These foam pieces were then compressed for a minimum of 72 hours before being pressed flat in the center of an alumina test crucible using a steel reshaping tool, just prior to testing. The temperature program included a 20-minute-long isotherm at 75°C followed by heating at a constant rate of 10 K/min to 700°C. Five replicate TGA tests were performed, and the average results were used to estimate kinetic parameters. The calibrated kinetic parameters are provided in Table 8. A plot of the experimental data along with the fit parameters is given in Figure 4. Again, the results predicted using the calibrated kinetic parameters agree quite well

with the TGA data. In fact the predicted peak mass loss rates for both reactions are approximately equal to the experimental values.

4.3 | Polyvinyl Chloride

PVC samples were obtained from Interstate Plastics (manufactured by Vycom plastics: Type 1 PVC) in the form of 6-mm thick slabs. For each test, small, flat pieces between 4.5 and 5.5 mg in mass, were carefully cut from these slabs and placed in the center of an alumina test crucible. The temperature program included a 30-minute-long isotherm at 40°C followed by heating at a constant rate of 10 K/minutes to 700°C. Six replicates were performed, and the average TGA signal was used to calibrate the kinetic parameters. The algorithm predicts a three-reaction mechanism, and the calibrated kinetic parameters are tabulated in Table 9. The data and corresponding fits are shown in Figure 5. It is apparent that the fit is not as good as was obtained for the other two materials. This can be attributed to the relative noisiness of the experimental data along with the fact that the first two reactions are relatively close to one another. However, the peak mass loss rates for all three reactions is very well captured by the calibrated kinetic model. The adequacy of this, or any fit, ultimately depends on the ability of the calibrated parameters to make accurate predictions of burning rate and flame spread in fire models. Such a study is beyond the scope of this paper.

Further validation of the algorithm has been performed for 11 different vegetative fuels.¹³ These vegetative fuels typically exhibited two to three reaction peaks within close proximity and with considerable noise in the data. As can be confirmed in the reference, the automated fitting algorithm described in this paper performed well even in these more challenging scenarios.

5 | CONCLUSIONS

A novel methodology has been presented for finding the kinetic parameters of pyrolysis from TGA data. The advantages of this algorithm are that (a) it is fully automated requiring no interaction from

the user, (b) it is computationally efficient in providing the kinetic parameters in less than 1 second, and (c) it has been verified and validated. The need for such a methodology is driven by a demand for material properties needed as inputs for fire models of flame spread.

Verification was performed by applying the algorithm to manufactured data for several one and two reaction pyrolysis mechanisms. As expected by the underlying theory, it was found that the algorithm performed better for narrower reactions. Additionally, slightly better fits were obtained for well-separated reaction peaks. For the two-reaction scenarios, it was found that the algorithm can sometimes fail to exactly predict mass plateaus between reactions. This is a consequence of the fact that the methodology focuses primarily on capturing the mass loss rate as opposed to the sample mass. A focus on the mass loss rate is justified since flammability is governed by the rate at which combustible volatiles are generated rather than the current amount of mass remaining in the sample. The results of the different verification cases demonstrate that even in situations in which the mass signal is not perfectly captured, the mass loss rate is quite accurate.

Three different materials were used to validate the algorithm: Nylon 66, PVC, and flexible PU foam. All TGA tests for these three materials were performed at a heating rate of 10 K/minutes in a nitrogen environment with the samples placed in an alumina crucible. These cases proved to be a rigorous test of the algorithm since the materials varied in the number of reactions predicted as well as the noise in the underlying data. Kinetic parameters for all three of these materials were determined using the automated algorithm, and the resultant model predictions agreed with the data nicely. A natural extension of this validation process is to test the derived kinetic parameters for TGA at different heating rates. It would be useful to explore the applicability of the calibrated kinetic parameters for making predictions of TGA at lower heating rates, and this remains an avenue for future work. However, a simple heat transfer analysis¹⁴ indicates that the validity of assuming a spatially uniform sample temperature breaks down for heating rates much greater than 10 K/minutes for typical TGA sample sizes. Consequently, data obtained at larger heating rates would include transient effects from thermal (and possibly mass) transport rather than just pyrolysis kinetics. Such a conflation of physical processes will likely inhibit the effectiveness of the derived parameters to make predictions of full-scale scenarios when used in conjunction with separately derived transport properties.

Although the algorithm has been verified and validated to some extent, more validation is always desirable in order to find the limits of applicability of the algorithm. The results presented in this paper are quite promising, but it would be desirable to make better fits for broader peaked reactions as well as for overlapping reactions that occur at very similar temperatures. Furthermore, as was seen in the validation cases, different materials can produce different amounts of noise in the raw TGA data. It would therefore be helpful to make the algorithm more robust against varying degrees of noise. These improvements are primarily related to the very first step in the algorithm which uses the Savitzky-Golay filter to smooth the data and find sufficiently smoothed derivatives. There are several parameters involved in this process that need to be optimized by further study.

Finally, the true test of the effectiveness of this novel methodology lies in its effectiveness at providing parameters that accurately predict burning rate and flame spread in fire models such as FDS. Future work will therefore involve developing similar procedures to use other micro-scale data such as DSC and microscale combustion calorimetry to estimate the other parameters needed in fire models. Once a more complete program of automation is achieved, it will be possible to validate the procedures by comparing fire model results with experimental flame spread data of real materials. Such a process will take significant effort, but the present paper provides a critical first step in this direction.

Disclaimer: The identification of any commercial product or trade name does not imply endorsement or recommendation by NIST.

ORCID

Morgan C. Bruns  <https://orcid.org/0000-0001-6101-4383>

REFERENCES

1. McGrattan KB, Hostikka S, McDermott R, Floyd J, Weinschenk C, Overholt K. *Fire Dynamics Simulator, Volume 1: Mathematical Model*. Vol 1. 6th ed. National Institute of Standards and Technology, NISTIR, Special Publication: Gaithersburg, MD; 2019:1018.
2. Lautenberger C, Fernandez-Pello C. Generalized pyrolysis model for combustible solids. *Fire Saf J*. 2009;44:819-839.
3. Stolarov SI, Lyon RE. Thermo-kinetic model of burning. Technical Report DOT/FAA/AR-TN08/17, Federal Aviation Administration; 2008.
4. Stolarov SI, Li J. Parameterization and validation of pyrolysis models for polymeric materials. *Fire Tech*. 2016;52:79-91.
5. McGrattan KB, Hostikka S, McDermott R, Floyd J, Weinschenk C, Overholt K. *Fire Dynamics Simulator: Technical Reference Guide, Volume 3: Validation*. Vol 1. 6th ed. Gaithersburg, MD: National Institute of Standards and Technology NISTIR, Special Publication; 2019:1018.
6. Brown A, Bruns M, Gollner M, et al. Proceedings of the first workshop organized by the IAFSS working group on measurement and computation of fire phenomena (MaCFP). *Fire Saf J*. 2018;101:1-17.
7. Bruns MC, Koo JH, Ezekoye OA. Population-based models of thermoplastic degradation: using optimization to determine model parameters. *Polymer Deg Stab*. 2009;94(6):1013-1022.
8. Bruns MC. Inferring and propagating kinetic parameter uncertainty for condensed phase burning models. *Fire Tech*. 2016;52(1):93-120.
9. McGrattan KB, Baum HR, Rehm RG, Hamins A, Forney GP. *Fire Dynamics Simulator: Technical Reference Guide, User's Guide*. 6th ed. National Institute of Standards and Technology, NISTIR, Special Publication: Gaithersburg, MD; 2019:1019.
10. Savitzky A, Golay MJE. Smoothing and differentiation of data by simplified least squares procedures. *Analyt Chem*. 1964;36(8):1627-1639.
11. NETZSCH. *Software Manual (STA 449 F1 & F3) Temperature and Sensitivity Calibration*. NETZSCH Gerätebau GmbH: Selb, Germany; 2012.
12. ASTM. *D3574-08. Standard Test Methods for Flexible Cellular Materials—Slab, Bonded, and Molded Urethane Foams*. ASTM International: West Conshohocken, PA; 2008.
13. Leventon IT, Bruns MC. Thermal decomposition of vegetative fuels. Paper presented at: Proceedings of the 15th International Conference and Exhibition on Fire Science and Engineering (Interflam); 2019; London, UK.
14. Lyon RE, Safronava N, Senese J, Stolarov SI. Thermokinetic model of sample response in nonisothermal analysis. *Thermochim Acta*. 2012; 545:82-89.

How to cite this article: Bruns MC, Leventon IT. Automated fitting of thermogravimetric analysis data. *Fire and Materials*. 2020;1-9. <https://doi.org/10.1002/fam.2849>